Optics design and performance for the Cosmic Hot Interstellar Plasma Spectrometer (CHIPS)

M. Sholl[a], B. Donakowski[a], G. Gaines[b], M. Lampton[a], M. Hurwitz[a], M.M. Sirk[a], E. Taylor[c]

[a]Space Sciences Laboratory, University of California, Berkeley CA, USA, [b]Gaines Systems, Berkeley CA, USA, [c]Design Net Engineering, Boulder CO, USA

ABSTRACT

The CHIPS observatory was launched on 12 January 2003, and is the first UNEX (NASA Goddard Spaceflight Center University Explorer class) mission. It is currently on-orbit and performing diffuse spectroscopy in the 90-260Å wavelength band. The instrument is integrated with a custom 3-axis stabilized mini-satellite, designed for roughly one year of operation. The purpose of the observatory is examination of details of the local bubble thermal pressure, spatial distribution and ionization history. The spectrometer consists of six spectrograph channels which deliver >λ/100 resolution spectra to a single detector. Cost constraints of UNEX led to a design based on a traditional aluminum structure, and an instrument with a large field of view (5º x 26º) for the dual purpose of increasing sensitivity in the photon-starved 90-260Å band, and to reduce requirements on spacecraft pointing. All optomechanical systems on the spectrometer, including coalignment, thermal, front cover and vacuum door release are performing well on orbit. We discuss design, test and operational performance of these systems, as well as launch loads and thermal system considerations.

Keywords: Shape Memory Alloy, Semi-Kinematic, Flexure, Zerodur, UNEX, CHIPS, Local Bubble

1. INTRODUCTION

CHIPS launched on a Boeing Delta-II 7320-10 from Space Launch Complex Two (SLC-2), Western Test Range (WTR, Vandenberg AFB), into a 94° retrograde, ~600km polar orbit. The observatory consists of the spectrometer, and a mini-satellite designed specifically for integration with the spectrometer. The integrated CHIPS observatory is qualified for a Delta-II launch in the lower station of a Reduced Height Dual Payload Attach Fitting (RHDPAF).

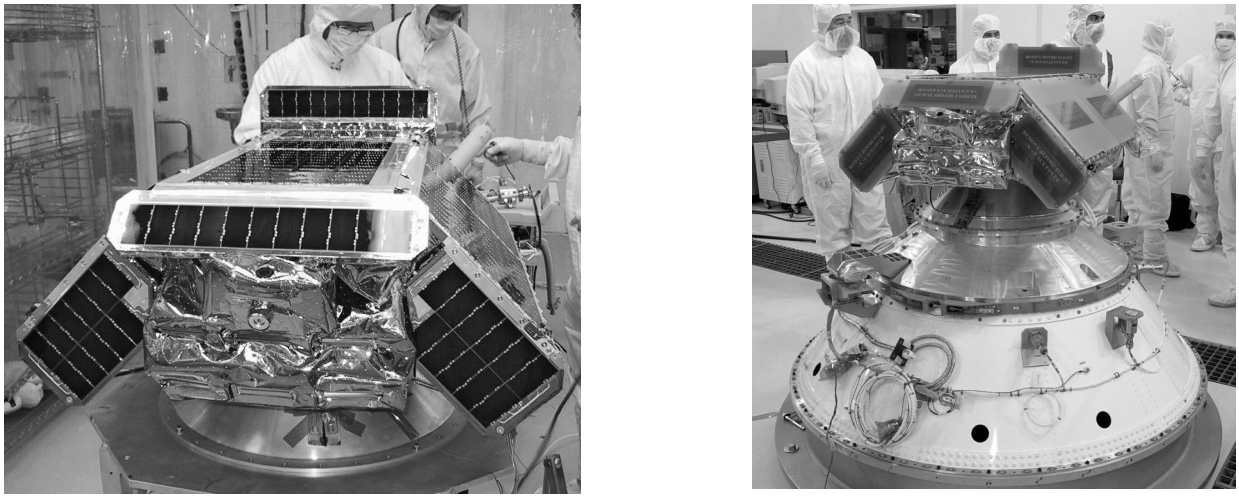

a b

Figure 1: Closeup of the CHIPS observatory (a), and CHIPS installed on the lower Payload Attach Fitting (PAF) of the Reduced Height Dual Payload Attach Fitting (RHDPAF)[1] (b).

The CHIPS instrument consists of six spectrometer channels which deliver extreme ultraviolet (EUV) radiation to a single microchannel plate (MCP) detector. The detector is detailed in a related paper by Marckwordt, et. al..[2] Light enters the system through narrow (250μm) or wide (1000μm) slits. Narrow and wide slits for each spectrograph channel are photoetched into a 1mm thick beryllium-copper sheet, and separated by ~1.6mm. The observer may select either slit via remote command to a slit wheel, which blocks the entrance path to either or both slits. The slit wheels are powered by a beryllium-copper rotary spring, and motion initiated by a shape memory alloy ratchet/pawl mechanism, as discussed in *Sholl, et.al.*.[3] Six identical slit mechanisms were fabricated and tested, and all were activated successfully twice, on orbit, at the time of this paper's publication. From the slit, light passes through a hole in the optical bench, and is dispersed by a cylindrical, rhodium coated, varied line spacing, reflective diffraction grating with a central line spacing of 1800 *rulings/mm.* First internal orders in the 90-260Å band form an image of the slit on the top microchannel plate. A NaBr photocathode, held at high negative potential produces a photoelectron when a photon arrives, and the electron cascades downward through a nearby microchannel due to a local electric field, eventually producing a cloud of ~10^7 electrons through secondary electron multiplication. The cloud is intercepted by a crossed delay line (XDL) anode, and a time to digital converter (TDC) quantifies the electron cloud position. Optical baffles are installed throughout the spectrometer (see Section 4). In order to avoid acoustic damage to the thin-film filters used for out of band rejection, the detector is launched in a sealed vacuum chamber. The detector vacuum chamber is designed to be ion-pumped until rendered inaccessible by launch vehicle encapsulation. On orbit, the door is opened via remote command to a shape memory alloy actuator. Design, testing and operation of the detector release mechanism are discussed Section 5.

2. THERMAL EXPANSION AND COALIGNMENT

Details of the optical prescription, and theoretical performance of the spectrometer are detailed in Sholl *et. al.*,[3] to which this should be considered a companion paper. This paper covers additional details not discussed in Sholl *et. al.* Figure 2a and 2b show the spectrometer layout, and a photo of the spectrometer prior to installation of multilayer insulation blankets (MLI).

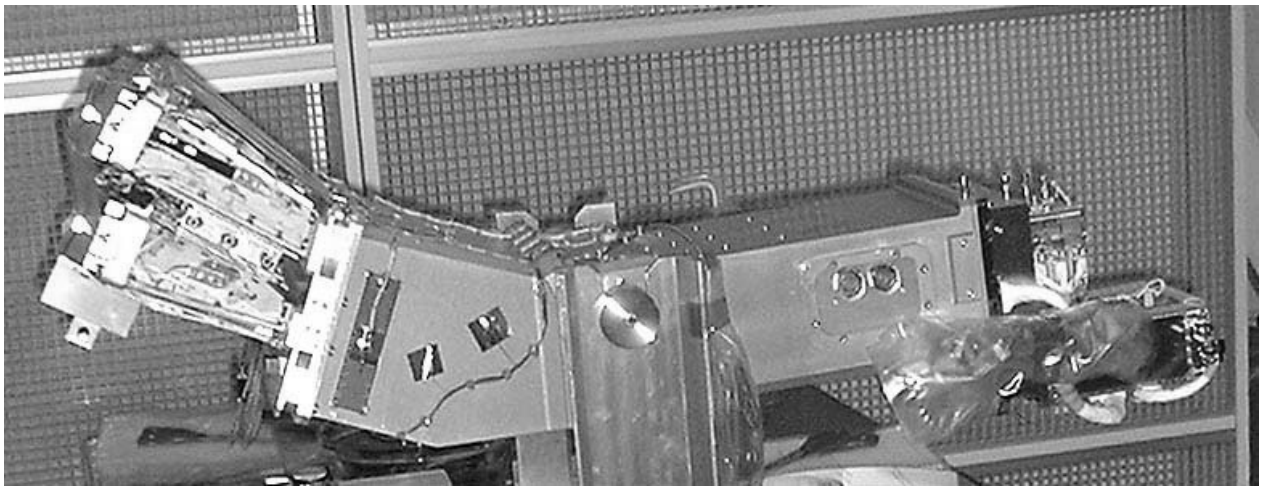

Figure 2a: Photograph of the spectrometer, prior to installation of multilayer insulation blankets. The main structure is a heavily weight-relieved aluminum shell.

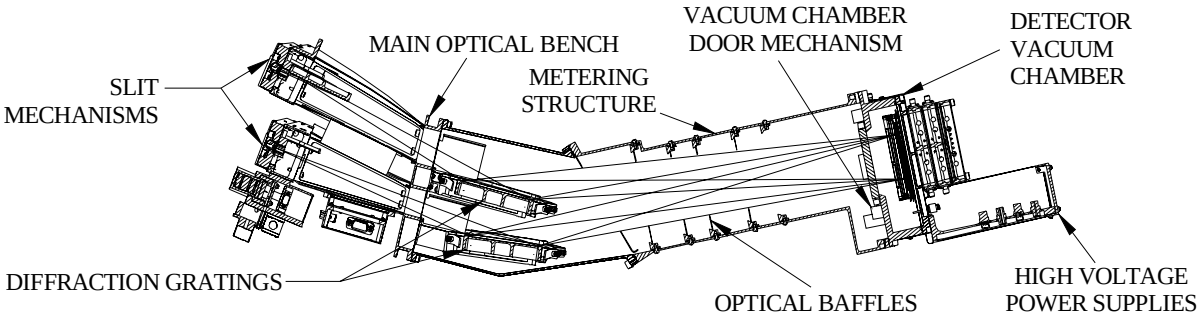

Figure 2b: Spectrometer configuration photo and cutaway view.

Among the challenges on CHIPS were initial coalignment of the spectrometer channels, and maintenance of coalignment in the presence of thermal gradients and launch dynamics. Each spectrometer channel is a relatively slow (*f*/14) optical system, and therefore optical misalignments on the order of the slit width are tolerable with small degradation in spectral resolution. Because the spectrograph combines slit images from six separate channels, slit images must be coaligned, and coalignment maintained, within a small fraction of their size on the focal plane (~250μm).

Initial alignment was achieved using 5mm visible ruling patches on the ends of the gratings. A HeNe laser was split into four beamlets by 25%, 33% and 50% reflection beamsplitters. Beamwalk mirrors were used to direct pairs of beamlets through the entrance slit, off the visible patches, to the focal plane at the cross-dispersion extremes of the detector. During visible light alignment, the detector was replaced with a ground glass surrogate detector, and a pair of CMOS cameras used to image the ground glass screen near the extremes of the spectral feature. A wire feducial mounted on the ground glass served as a coalignment target. The alignment technique is beyond the scope of this paper, but based on recognizing optical distortion and misalignment by the differences in the "speed" of motion of the near and far visible patch spots, on the focal plane, for a given grating angular motion. Initial alignment was achieved when all four spots were positioned on the wire. Fine alignment was performed with removable 80 thread per inch micrometers, based on measurements made at EUV wavelengths in the vacuum calibration facility.

Lateral motion of any slit image degrades the spot size in direct proportion to the image motion (see Figure 3c). For an aluminum structure (CTE=23.6 ppm/°C), and the original nine-channel spectrometer design, a 10°C shift in the temperature of the slit plane relative to that of the grating plane results in a 30% degradation in spectral resolution. Graphite Epoxy and Super Invar have CTEs of 0 and 0.3 ppm/°C respectively[4], and their use in the slit plane design would reduce the spectral resolution degradation to negligible levels, but only with a significant increase in fabrication complexity, time and cost (as well as mass, in the case of Super Invar). Due to the cost and schedule constraints of the CHIPS mission, an all-aluminum structure was baselined. In order to minimize lateral slit shift while using an all-aluminum structure, slits and gratings are mounted on cantilevers which extend in directions roughly normal to the optical bench surface (see Figure 3). The optics bench is an effective center of expansion, and the slits and gratings move along *slow* optical axes when an axial gradient is applied (Figure 3d). Lateral (left to right in Figure 3) thermal gradients cause the optics bench to undergo solid body rotation, and the image is shifted without noticeable degradation. A design goal was to keep lateral thermal gradients transients below 2ºC (steady thermal shifts are acceptable, but time-varying shifts caused by passage in and out of Earth's shadow complicate data analysis, and are not desirable).

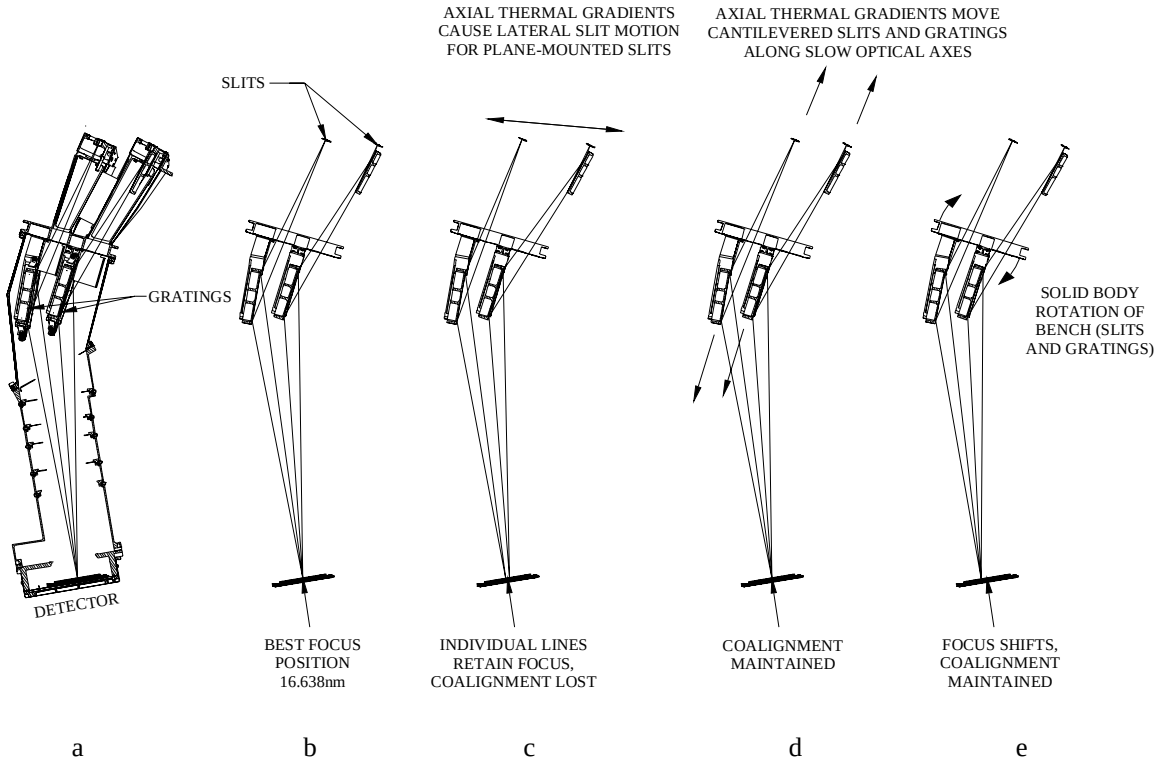

Figure 3: Effects of thermal gradients on spectral resolution. Axial thermal gradients cause slits (and detector slit images) to move apart when slits are mounted on a common plane (c). Cantilevered slits and gratings (d) move along their optical axes when exposed to an axial temperature gradient. For slow systems such as the *f*/14 spectograph channels, this does not degrade performance significantly. Lateral thermal gradients across the metering structure translate spectral feature locations, but do not degrade spectral resolution (e).

The spectrometer is packaged tightly between a hot (70ºC) solar array and a cold (10ºC) spacecraft electronics radiator. To minimize gradients, the metering structure was made of aluminum, and wrapped by two five-layer MLI blankets (effective emissivity: <0.05). Compared with temperatures measured across the metering structure during vacuum calibration, less than a 0.5°C lateral thermal gradient is introduced by on-orbit thermal loading. Spectral features are shifted by 1.1Å compared with vacuum tank measurements, and this shift is not explained by the presence of a thermal gradient. By design, both the spectrometer and the electronics box experience lower temperatures on-orbit than they did during vacuum calibration, and this may account for the difference in the position of the spectral features. The offset is well-quantified, and may be subtracted from measured photon positions due to the effect's temporal invariance.

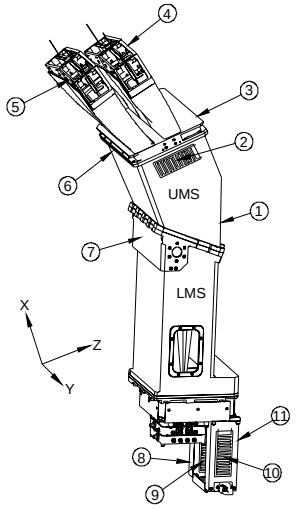

#	Location	Face	Type[a]	Min[b]	Max[b]
1	Upper metering structure (UMS)	+Z	T	11.9	12.9
2	Optics bench 1	+Y	T, H	11.2	12.2
3	Optics bench survival heater	+Z	T, H	11.6	11.9
4	North tower slit survival	+Z	T	10.0	11.8
5	South tower slit	-Z	T	7.4	9.5
6	Optics bench 2	-Y	T, H	11.2	12.2
7	Lower metering structure (LMS)	+Y	T	11.2	13.6
8	HVPS 0 survival heater	-Y	T, H	11.2	13.1
9	HVPS 0	+Y	T, H	11.2	13.6
10	HVPS 1 survival heater	+Y	T, H	9.9	11.8
11	HVPS 1	-Y	T, H	9.5	12.2

a: T=Thermistor, H=heater b: typical values (°C) while observing

Figure 4: Location of heaters and thermistors on the spectrometer. Typical Min/Max temperatures throughout observing day.

3. STRUCTURAL DYNAMICS AND COALIGNMENT

The aluminum shell metering structure performed well under protoflight dynamic loading conditions. One early concern involved the cantilevered high voltage power supplies (HVPS), which are mounted directly on the detector housing (See Figure 2b). This configuration was adaped by using ORFEUS heritage Spacom HVPSs modified with a direct-mount connector designed for the IMAGE program. The design eliminates HV cabling, and eliminates one HV connection per supply (considered a technical risk). The cantilevered, direct mount HVPSs performed flawlessly during environmental testing and on orbit.

The detector, slit mechanisms, vacuum box door mechanism and metering structure, all new designs, were qualified successfully. The main structural design issue encountered during CHIPS development involved the cantilevered grating mounts. Each grating has distinct lateral and torsional modes with frequencies in the 170Hz to 300Hz band. Early random protoflight spectra levied on the CHIPS spectrometer called for testing at an acceleration spectral density of $0.14g^2$/Hz across this band. Levels were derived from the Delta-II Secondary Payload Planners Guide[5] (SPPG), with additional margin based on early predictions of the spacecraft dynamics. Due to the low output impedance of the vibration table and high dynamic amplification factor of the grating mounts (as high as ~30), grating contact and coalignment degradation were observed during early shake tests. Clearances between adjacent channels are as small as 3.0±0.5mm (see Figure 5). Grating mounts were stiffened by increasing the thickness of mounting posts (using a finite element model of the optics bench, grating mounts and slit towers) until a point of diminishing return in frequency increase was reached. Additionally, area moment balancing gusset plates (Figure 5b) were added to the open front face of the grating mount brackets.

Because launch loads are lower for a secondary payload flying in a dual payload attach fitting (compared with loads experienced on the Delta-II secondary payload envelopes SPE1 and SPE2, described in the Secondary Payload Planners Guide) test levels were reduced from those required by the SPPG to a RHDPAF specific $0.02g^2$/Hz (see Figure 6 for qualification loads). After assembly of the viton grating mounts (see Sholl, *et. al.*), a settling shake was performed, followed by channel coalignment, protoflight testing and a post-test coalignment verification in the vacuum calibration chamber. Subsequent to observatory qualification testing and launch, a 256Å helium airglow line was used to verify coalignment. A measured 76% energy width suggests a resolving power (based on Rayleigh's criterion) of ~120 on orbit—well within requirements. See Sirk, *et. al.*,[6] for a detailed analysis of spectrometer performance.

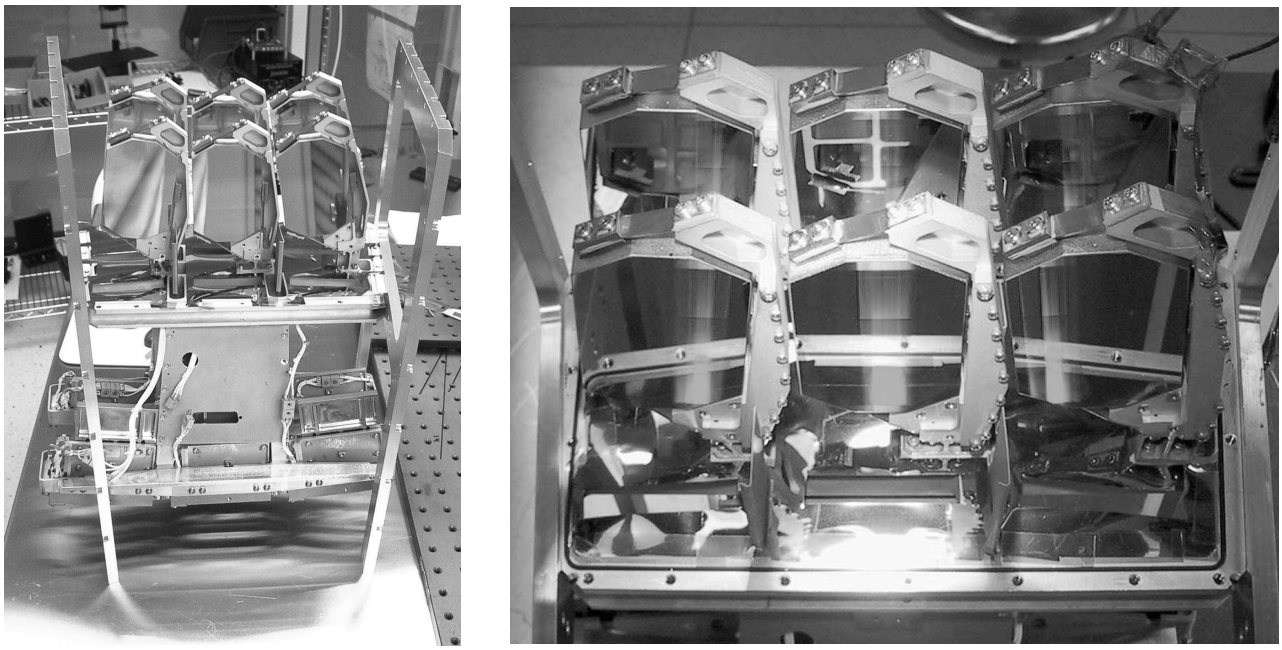

a b

Figure 5: Main optical bench. Six open back Zerodur gratings are cantilevered off the optics bench via aluminum pedestals. Individual gratings are isolated from the aluminum structure (aluminum and Zerodur have a CTE mismatch of ~20) via triads of tangentially oriented, 1mm thick beryllium copper blade flexures. Spectrograph channels are replicated by Euler rotations about the detector dispersion axis and the 166.38Å theoretical system centerband spectral feature. Channels are packaged as tightly as possible without mechanical or light path interference between channels (note the dogleg in the flexures, and the image of the weight relieved Zerodur in the back row gratings). Crosstalk baffles (Section 4) are visible near the bottom of Figure 5b.

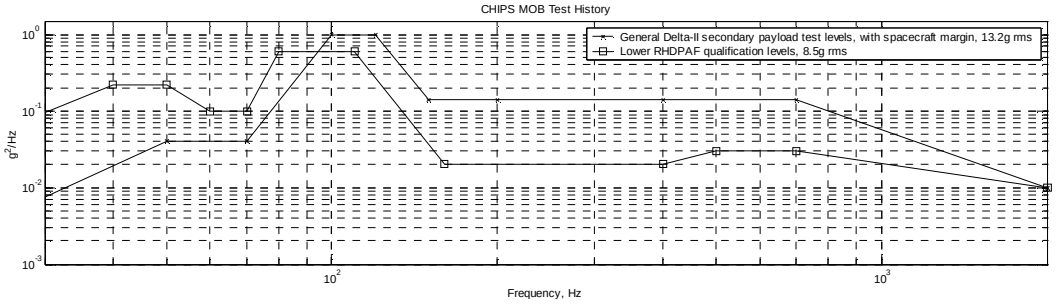

Figure 6: Protoflight random test levels. This figure shows the original test level, derived from the Delta-II SPPG, with margin added based on early predictions of spacecraft dynamics. Because payloads launched in a dual payload attach fitting (DPAF) experience lower random vibration levels than those experience in secondary payload envelopes as SPE1 and SPE2[5], the observatory qualification level was reduced to a lower DPAF-specific spectrum.

4. OPTICAL BAFFLE DESIGN

Optical baffles are placed in obvious locations throughout the instrument, and are added in several locations to correct effects discovered during testing. Figure 7 shows one such addition, a pair of baffles added to the pickoff mirror channels, designed to block an undesirable direct path (not reflected off the pickoff mirror) to the gratings. Figure 8 shows installation of an aluminized Mylar sheet on the upper surface of the optics bench. Custom holes (with geometries determined by raytracing and the Euler rotations of the individual spectrograph channels) are designed in CAD, cut into the sheet, and installed on the oversized Cartesian holes in the optics bench. This baffle effectively isolates the bright slit tower cavity from the darker grating cavity (below the optics bench), and eliminates the majority

of stray light issues revealed by early testing. After visible ruling alignment (see Sholl, *et. al.* for a description of the visible rulings), visible patches are shaded by aluminized Mylar sheets. The optics bench baffle blocks the path between the entrance slits and the visible ruling patch nearest to the optics bench. The visible patch closest to the detector is blocked via application of aluminized Mylar directly to the lower edge facet of the gratings.

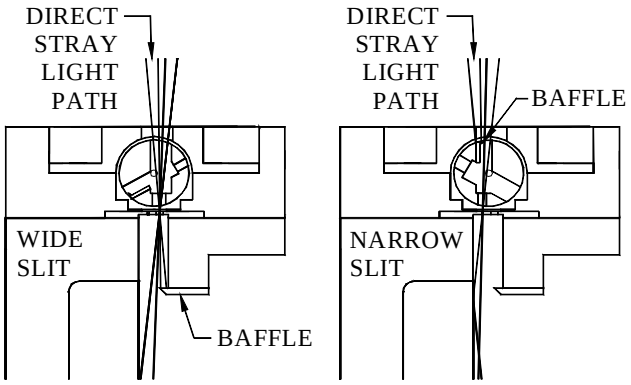

Figure 7: Direct path optical baffles

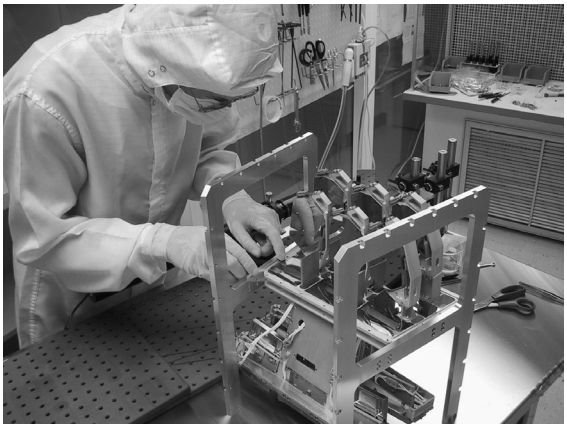

Figure 8: Installation of optics bench baffle

CAD visualization of the spectrometer indicated possible cross-channel illumination paths through the optics bench. These paths were blocked using crosstalk baffles (See Figure 9, crosstalk baffles are also visible in Figures 5 and 8). Metering structure baffles are shown in Figure 2b. These baffles are bead-blasted, anodized aluminum sheets, positioned to block midfield light outside the geometric path from the grating perimeters to the active detector area. The inner surface of the vacuum box door contains integral baffle vanes to stop zero-order light from reflecting off the open door into the detector. A PEEK plastic baffle sits directly above the filter frame panel (Figure 10), and acts as a last line of defense against stray radiation.

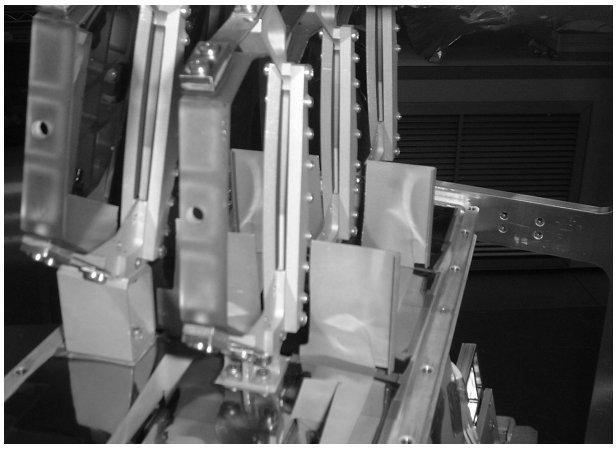

Figure 9: Channel crosstalk baffles

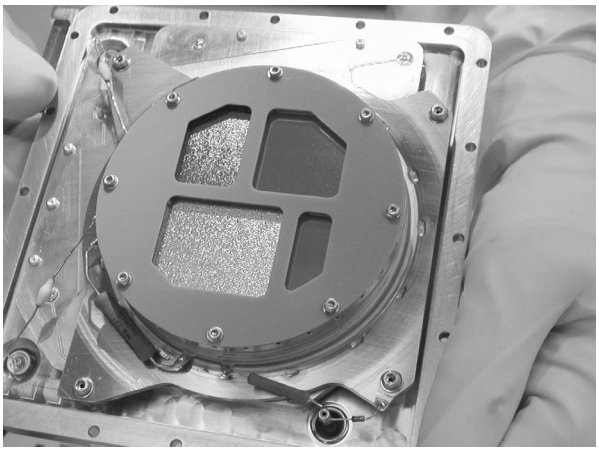

Figure 10: Detector baffle

Figure 11 is an on-orbit detector image from CHIPS. He II (Lyman β and γ, 256Å and 243Å, respectively.) are visible near the right (high wavelength) end of the image. These lines are useful for verification of wavelength scale and channel coalignment. Detector hot spots are visible in the lower right quadrant. Hotspot data are eliminated for data analysis. Several artifacts appear in the lower left quadrant, after very long integration. One possible origin is Lyman α (1216Å) scattering off the bottom of the slit wheel, passing through both slits, and diffracted (high orders) off one of the visible rulings. Slit wheels are effectively thermally decoupled from the main structure by ball bearings, and were therefore gold (which scatters Lyman α) plated to reduce radiation to deep space.

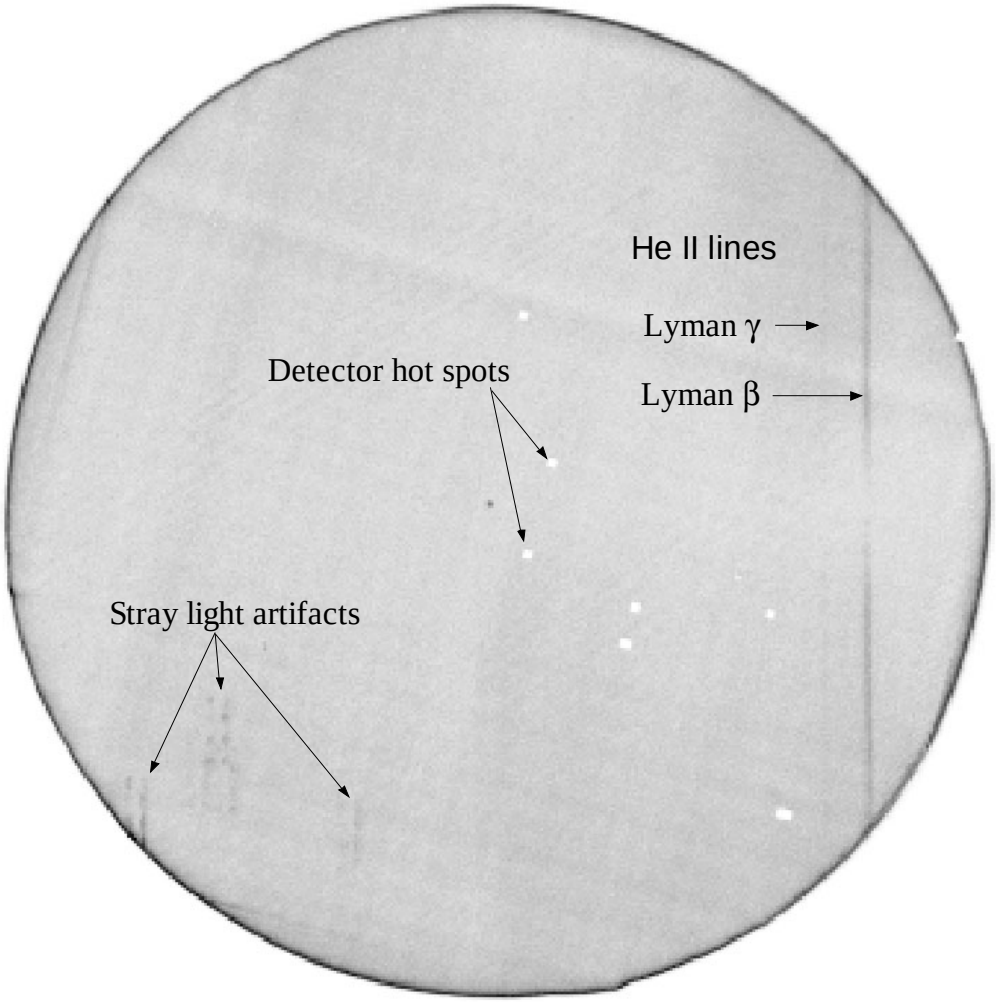

Figure 11: Narrow slit detector image shows coaligned spectral features He II (Lyman β: 256Å and Lyman γ: 243Å), detector hot spots (removed from telemetry), and possible stray light artifacts visible during long integrations.

5. DETECTOR VACUUM CHAMBER DOOR

The detector must be stored at vacuum for the following reasons:

- Preserve the extremely hygroscopic NaBr photocathode
- Preclude thin metal filter damage by launch and qualification acoustic energy
- Preserve the low microchannel plate background level (increases if stored at ambient pressure)
- Protector from gas inrush when vacuum calibration facility is vented to air

Due to the small size of the optics chamber, mass constraints, and a desire to reduce complexity of on-orbit operations, a one-shot release mechanism was baselined to actuate the vacuum chamber door. Shape memory alloy actuators were chosen to release the mechanism, primarily because of their large stroke (2.5cm), adequate force (>5N), low mass, low cost and high reliability (a test actuator was subjected to >100,000 loaded cycles). A four-bar linkage mechanism was used to open the vacuum box door (after first actuating the flight door latch) and close it at the end of each vacuum test. The O-ring requires ~400N, applied at the center of the door, to create a vacuum seal, and the mechanism was therefore designed with a high-torque gearmotor. High forces generated by this mechanism could easily damage the spectrometer or injure nearby personnel, so the mechanism and controller were designed for fail-safe operation. The system is driven by a microcontroller circuit which monitors multiple limit switches, and the motor may be run backwards or beyond the limit switches without damaging hardware. The mechanism is attached to the door via a "fork" which can only push on the door (see Figure 13). If an operator commands the mechanism to open the door before releasing the flight latch, the fork falls away from the door without causing damage the latch mechanism. Using this GSE, vacuum calibration was completed without incident, and the four-bar interface removed from the spectrometer prior to instrument closeout.

Shape memory alloy actuators were Coulomb heated to their transition temperature by a current drawn directly from the spacecraft batteries (no switching converters or heaters were used in the circuit). Two enable FETs and a mechanical enabling plug (installed at Vandenberg, prior to launch vehicle encapsulation) were connected in series with the circuit to prevent inadvertent actuation. A pulse width modulation driver was not implemented, and due to the low resistance (~0.25Ω) of the actuators, a 2.5Ω shunt resistor was placed in series with the circuit to maintain harness current levels within GSFC recommended de-rate levels. Spacecraft and instrument electronics were designed to power either actuator individually, or both at the same time in the event of a stuck mechanism. Actuators are driven by a 4A current for 10s. This interval was determined from a finite difference thermal model of the actuator, and actuation verified at high and low temperature extremes while powering the actuators through flight circuitry at the high and low spacecraft battery charge voltages.

A pair of actuators is attached by cable to a force doubling bellcrank (see Figures 12-14). The short arm of the bellcrank is attached by cable to the torsion spring biased, graphite dry-film coated, primary release latch (see Figure 12), which through mechanical advantage and the low-friction coating provides a force multiplication factor of 10. The secondary and tertiary latches are biased against the primary latch by a stainless steel tongue (rod) force fit into the free end of the door. O-ring preload and the hinge-mounted door release spring provide the tongue biasing force against the tertiary. The secondary and tertiary latches provide a further force multiplication factor of 10 from the primary latch to the door tongue.

After actuation, the door swings open and is stopped by a polymer block on the metering structure. The entire actuation process usually lasts 3-4s. The underside of the vacuum box door has integral bead-blasted anodized aluminum baffles to prevent zero-order light from reflecting off the door into the detector.

In order to reduce the risk of O-ring stiction, the O-ring was coated with a thin layer of Apiezon L vacuum grease. The tertiary was loaded by a linear spring, and had an integral "heel" designed to force the door open in the event of O-ring stiction. The O-ring was captivated in the door by a dovetail groove. Dissimilar materials were used throughout the design (phosphor bronze, aluminum, stainless steel, PEEK) in order to reduce the risk of galling on orbit. Loose diametral tolerances (~25μm) and Braycote 601 lubricant were employed on all moving shaft interfaces.

Door position was sensed by a pair of potentiometers located collinearly with the door axis. The potentiometers were coupled to the door via a clearance fit coupling fork (see Figure 12), and read out by the spectrometer housekeeping system.

On orbit, the primary actuator was selected, and the door opened without incident.

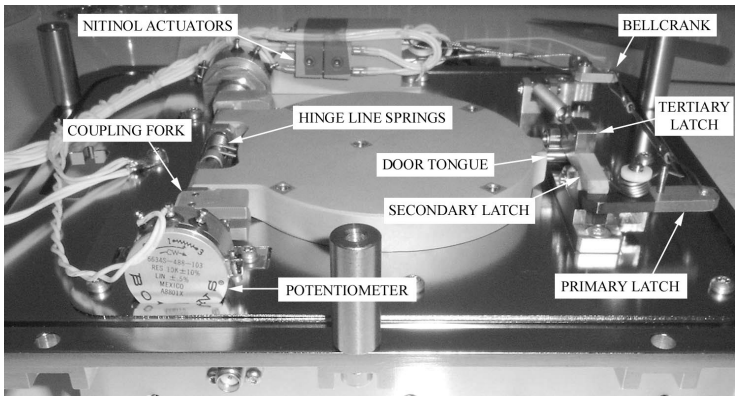

Figure 12: One-shot release door mechanism. The vacuum chamber door is spring loaded, and opened on-orbit by Coulombic heating of a shape memory alloy (nitinol) actuator.

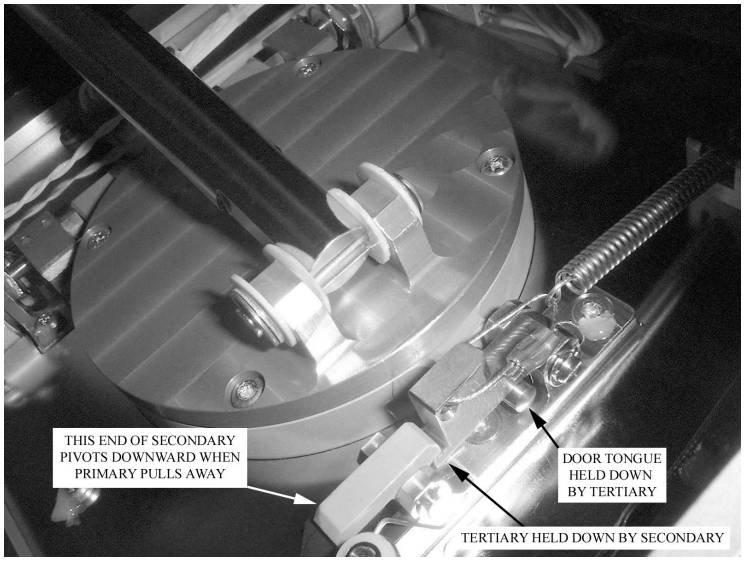

Figure 13: The one-shot door release mechanism allows the door to be opened, but has no provision for closing the door subsequent to actuation. The door must be closed prior to venting the vacuum calibration facility to ambient. During vacuum calibration, a four-bar linkage GSE (note stainless steel bar in photo) is employed to open and close the chamber door.

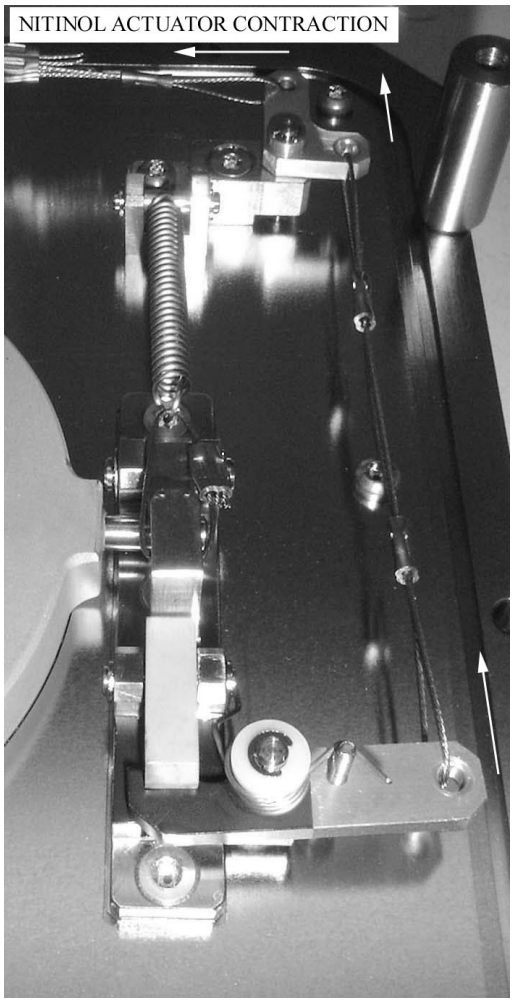

Figure 14: Mechanical advantage gain. The Al bellcrank (top) and primary (bottom) trade actuator stroke for force[7] (factor of three total). PEEK plastic secondary and tertiary multiply forces by an additional factor of 10, producing 180N of force at the door tongue to compress the O-ring. Sliding surfaces on the primary latch are coated with a dry film graphite layer.

6. CONCLUSIONS

CHIPS is a NASA/Berkeley University Explorer mission launched on 12 January 2003. It is currently performing diffuse EUV spectroscopy in the 90-260Å band. Coalignment of the six spectrograph channels was achieved during calibration, and maintained during observatory qualification and launch. Sensitive coalignment parameters were

identified, and an all-aluminum structure designed to maintain coalignment in the presence of the large gradient between the solar array and electronics radiator. Grating coalignment was maintained during qualification and launch. Thermal gradients across the metering structure were measured <0.5ºC, well within requirements, on orbit. The optical baffle system consists of aluminum plates, aluminized mylar sheets and a PEEK detector baffle. The aluminized mylar baffle on the optics bench, which separated the slit towers from the metering structure cavity, eliminated the majority of stray light problems observed during vacuum calibration. Residual stray light artifacts are possibly from stray Lyman α diffracted in high order from the visible ruling patches. Six shape memory alloy actuated slit mechanisms and the one-shot vacuum chamber door were designed and qualified for the CHIPS mission. All performed flawlessly on orbit.

ACKNOWLEDGEMENTS

This work was supported by NASA grant NAG5-5213. Ron Bettini and Kevin Kim (Swales Aerospace) developed the highly effective thermal design for the CHIPS observatory. Slit mechanisms were designed by Jeremy McCauley, the vacuum box door release mechanism by Karl Kromer, and the four-bar vacuum box GSE by Ken McKee. Jonathan Wolff (SpaceDev Inc.) designed the spacecraft electronics system, and Jane Hoberman led the design effort on the spectrometer electronics. The support of GSFC personnel, in particular David Pierce, was instrumental in the development of the CHIPS observatory.

REFERENCES

1. Photo source: http://mediaarchive.ksc.nasa.gov/search.cfm?cat=89
2. M. Marckwordt, G. Gaines, J. Edelstein, R. Hemphill, J. Hoberman, J. Hull, M. Hurwitz, M. Lampton, W. Marchant, K. McKee, T. Sasseen, M. Sholl, O. Siegmund, M. Sirk, D. Stone, E Taylor, "The EUV detector of the Cosmic Hot Interstellar Plasma Spectrometer" *Proc. SPIE* 5164-07, 2003.
3. M. Sholl, W. Donakowski, M. Sirk, T. Clauss, M. Lampton, J. Edelstein, M. Hurwitz, "Optomechanical design of the cosmic hot interstellar plasma spectrometer (CHIPS)" *Proc. SPIE* 4854, 465-478, 2002
4. Yoder, P. *Opto-mechanical Systems Design*, 127, Marcel Dekker, Inc., 1993.
5. Delta Launch Vehicle Secondary Payload Planner's Guide for NASA Missions, NASA Kennedy Spaceflight Center, Expendable Launch Vehicle (ELV) Services, September 1999.
6. M.M. Sirk, G. Gaines, E. Taylor, M. Sholl, W. Marchant, R. Hemphill, R. Kimble, T. Sasseen, M. Marckwordt, W. Donakowski "Performance of the Cosmic Hot Interstellar Plasma Spectrometer" *Proc. SPIE 5164-08*, 2003
7. K. Kromer, "CHIPS Prototype Detector Door Design Review" Internal review, 17 February 2000.

This work was supported by the Office of Space Sciences, National Aeronautics and Space Administration, under Grant No. NAG5-5219.

Contact: sholl@ssl.berkeley.edu; tel. 510 486-6340; Space Sciences Laboratory, 7 Gauss Way, Berkeley, CA 94720-7450 USA.